

# Control allocation for a high-precision linear transport system

R. Beerens<sup>1</sup>, S.C.N. Thissen<sup>2</sup>, A. van der Maas<sup>2</sup>, W.C.M. Pancras<sup>3</sup>,  
T.M.P. Gommans<sup>4</sup>, N. van de Wouw<sup>1,5</sup>, W.P.M.H. Heemels<sup>1</sup>

**Abstract**—We present a control allocation framework to improve the performance of an industrial translational transport and positioning system, based on an inverted permanent-magnet linear synchronous motor. Compared to the state-of-practice control solution, the proposed allocation technique achieves enhanced tracking, improved motion freedom, and relaxed hardware design specifications.

## I. INTRODUCTION

In this paper, we present a control allocation framework to improve the performance of industrial high-precision transport and positioning systems, see Fig. 1. In particular, we consider linear (i.e., translational) motion systems, where multiple carriers can move on horizontal tracks, using the *inverted permanent-magnet linear synchronous motor* (IPMLSM) actuation principle, see, e.g., [1]. Here, the coils of the three-phase actuators are located on the tracks and the magnets on the carriers, see Fig. 1, such that the moving carriers do not have any electronics or cables attached to them. This principle makes the system highly suitable to be used in automated production lines consisting of, e.g., operation in vacuum, high temperature, or chemical environments. Due to these characteristics, such systems are widely used in industry in, e.g., the production of flat screens, OLED lighting, and solar cells, see, e.g., [2]. The different operations that are executed on the products along the production line, requires the system to allow for flexible, and independent motion of each carrier along the track.

IPMLSM-based motion systems are typically over-actuated, since a carrier may commute with more than one set of coils in the track at the same time (i.e., one carrier is actuated by multiple actuators simultaneously), or multiple carriers may be influenced by the same set of coils (actuator) simultaneously. This may lead to conflicting control objectives, and may result in large position errors or

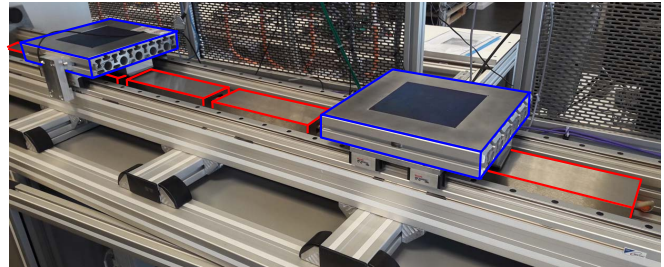


Fig. 1. Industrial IPMLSM-based transport and positioning system. The carriers are indicated in blue, and the actuators in red.

the inability to control carriers independently when using state-of-practice control solutions. Moreover, the actuator characteristics suffer from position dependency and end-effects (to be discussed in more detail in Section II), which pose design limitations in the sense that actuators must be placed at specific locations on the tracks. In this work, we aim to overcome the above limitations by means of intelligent (allocation-based) control.

IPMLSM-based transport systems are often controlled using Field Oriented Control, see, e.g., [3], [4], where actuator redundancy is often handled through the use of commutation algorithms [1], [5]. These algorithms aim to find a linear combination of all control inputs acting on a carrier, such that only a force in the direction of motion is generated. However, these existing commutation algorithms cannot handle independent control of multiple carriers simultaneously. Other control techniques that can handle actuator redundancy are, e.g., optimal control (see, e.g., [6], [7]) or control allocation (see, e.g., [7], [8]). Well-known examples of the former are linear quadratic control [6, Ch. 15], [9],  $\mathcal{H}_\infty$  control [6, Ch. 16-18], or model predictive control [10].

For the current application, however, control allocation techniques offer several benefits over other techniques: it may invoke less computational efforts compared to optimal control techniques [7], and separates controller tuning from the distribution of the resulting control efforts. In this way, well-known loop-shaping techniques often used in industry for the tuning of motion controllers can still be applied.

In this paper we present a control allocation framework for an IPMLSM-based transport and positioning system that achieves 1) increased tracking performance compared to industrial, state-of-practice control solutions, 2) independent motion of carriers, and 3) a relaxation of hardware design restrictions. The remainder of this paper is organized as follows. In Section II, we provide a detailed system description, and the proposed control allocation architecture is discussed in Section III. We illustrate the achievable performance

\*This research is part of the research programme High Tech Systems and Materials (HTSM), which is supported by NWO domain Applied and Engineering Sciences and partly funded by the Dutch Ministry of Economic Affairs.

<sup>1</sup>R. Beerens, N. van de Wouw, and M. Heemels are with the Dept. of Mechanical Engineering, Eindhoven University of Technology, P.O. Box 513, 5600MB Eindhoven, the Netherlands, {r.beerens; n.v.d.wouw; w.p.m.h.heemels}@tue.nl

<sup>2</sup>S. Thissen and A. van der Maas are with ASML, De Run 6501, 5504DR, Veldhoven, the Netherlands, {stijn.thissen; annemiek.vandermaas}@asml.com.

<sup>3</sup>W. Pancras is with Fontys University of Applied Sciences, Dept. of Mechatronics, P.O. Box 347, 5600AH Eindhoven, the Netherlands, w.pancras@fontys.nl

<sup>4</sup>T. Gommans is with Microsure, Science Park 5080, 5692EA Son, t.m.p.gommans@tue.nl

<sup>5</sup>N. van de Wouw is also with the Department of Civil, Environmental and GeoEngineering, Univ. of Minnesota, USA, and with the Delft Center for Systems and Control, the Netherlands.

benefits of the proposed controller by a simulation study in Section IV, and provide conclusions in Section V.

## II. SYSTEM DESCRIPTION

This section starts with the basic actuation principle of an IPMLSM, followed by a model of the considered transport system.

### A. Actuation principle

In PMSM-based motion systems, the required three-phase currents to obtain the desired motion profile are typically generated in the so-called  $dq0$ -reference frame (see, e.g., [4, Ch. 6], [11, Ch. 10]), to simplify the control problem, see Fig. 2. The three-phase currents  $i_a$ ,  $i_b$ , and  $i_c$  (red) can be mapped onto the stationary  $\alpha, \beta$ -frame (blue) via the Clarke transformation [11, Ch. 10]. Next, the coil currents expressed in the  $dq0$ -frame are obtained by rotating the  $\alpha, \beta$ -frame by an angle  $\theta$ , (referred to as the *commutation angle*), i.e., the Park transformation [11, Ch. 10]. The coil currents are now expressed by the *direct current*  $i_d$  and *quadrature current*  $i_q$  (green). In a rotary PMSM, the quadrature current  $i_q$  is the only torque-generating current by straightforwardly matching the commutation angle to the angle of the rotor. The direct current  $i_d$  is then controlled to zero at all times, such that only one input signal (i.e.,  $i_q$ ) needs to be generated to achieve the desired motion.

In a *linear* (i.e., translational) inverted PMSM, the same principle can be applied by describing the commutation angle  $\theta$  as a function of the carrier position. Due to the fact that the stator is segmented into groups of three-phase coils, however, an inverted PMSM suffers from end-effects: there exist regions where the electronics in the tracks partially overlap a magnet array on a carrier. The correct commutation angle (i.e., such that  $i_q$  indeed implements the desired force on the carrier) is then a *nonlinear* function of the carrier position. The motor gain (i.e., the gain between the applied quadrature current and resulting force on the carrier) thus depends on the carrier position and the commutation angle. The segmentation of coils also gives rise to the following control problems. Firstly, carriers may be influenced by either one or two sets of coils (from now on referred to as “actuators”), leading to an over-actuated system. Secondly, actuators may also influence multiple carriers at the same time. However, since an actuator is only able to implement a correct commutation angle (and thus a correct control force) for a single carrier, the other one experiences large disturbance forces as a result of the difference between the desired and attained control force. This restricts the freedom

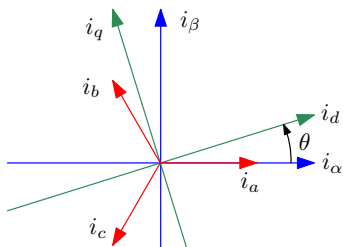


Fig. 2. Current reference frames for PMSMs.

in motion, in the sense that two adjacent carriers cannot perform an independent motion, as we will illustrate in Section IV.

Besides the aforementioned motion restrictions, an inverted linear PMSM suffers from hardware restrictions. The spacing between actuators has to be specifically related to the length of the magnet array on the carrier to achieve a smooth transition of a carrier between two actuators, see Fig. 3 (where we assume that the magnet arrays cover the full carrier length). In particular, the center distance of two actuators must be equal to the length of the magnet array  $L$ . When using this spacing, the motor gains of the actuators are constant for all carrier positions. Then, if the same quadrature current  $i_q$  is applied to multiple actuators, the applied force is independent of the carrier position. That is, there is no difference in the applied force to a carrier, regardless of whether the carrier is influenced by either one or two actuators. In this way, a single carrier may indeed be controlled accurately when actuated by multiple actuators (but does not allow for the control of multiple neighbouring carriers by the same actuator). This strict placement of actuators may be disadvantageous from an economic perspective. Namely, allowing for an increased spacing between actuators requires less actuators on the tracks, thereby reducing costs.

Summarizing, an IPMLSM-based motion system has the following limitations:

- Interaction of multiple carriers with one actuator results in conflicting control objectives and, consequently, may lead to large position errors or the inability to perform independent motions of the carriers;
- Interaction of a carrier with multiple actuators results in an over-actuated system, which is not explicitly addressed by the state-of-practice control solution;
- No freedom in actuator spacing to ensure a smooth transition of a carrier between actuators.

To address these limitations, we propose a control allocation framework in Section III that results in 1) enhanced tracking performance, 2) allowing independent motion of multiple carriers, despite the conflicting control objectives, 3) reduces power consumption, and 4) relaxed hardware design specifications.

### B. Carrier transport system modeling

Consider an IPMLSM-based carrier transport system consisting of  $n$  carriers and  $m$  actuators, see Fig. 3. Let  $j \in \bar{n} := \{1, 2, \dots, n\}$  be the carrier number, and  $k \in \bar{m} := \{1, 2, \dots, m\}$  the actuator number, used to uniquely identify all carriers and actuators in the system. The carrier transport system is governed by the dynamics

$$M\ddot{y} = B(y)u, \quad (1)$$

where  $y = [y_1, \dots, y_n]^T$  a vector containing the position of the carriers,  $M = \text{diag}(M_1, \dots, M_n)$  the mass matrix containing the individual carrier masses. In this work, we consider the  $\alpha, \beta$ -currents for each actuator as control inputs, instead of the frequently used  $i_q$ -current of the  $dq0$ -frame. Using the fixed  $\alpha, \beta$ -frame is advantageous for control allocation, because the commutation angle  $\theta$  then does not

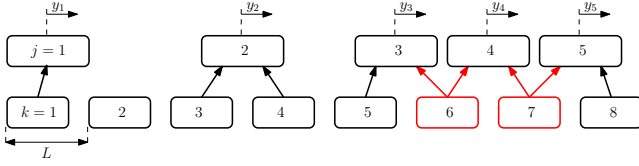


Fig. 3. Schematic representation of the IPMLSM-based transport system. Arrows denote the influence of an actuator (index  $k$ ) on a carrier (index  $j$ ), and arrows marked in red influence two carriers. .

appear in the motor gain matrix  $B(y)$  in (3) below. This is an instrumental observation for the proposed control solution (see also Remark 2 below). The input vector  $u$  is then given by

$$u = [i_{\alpha,1}, i_{\beta,1}, \dots, i_{\alpha,m}, i_{\beta,m}]^T. \quad (2)$$

Due to the position dependency of the commutation between the carriers and the coils, the motor gain matrix  $B(y)$  is given by

$$B(y) = \begin{bmatrix} b_{11}^{\alpha}(y_1) & b_{11}^{\beta}(y_1) & \dots & b_{1m}^{\alpha}(y_1) & b_{1m}^{\beta}(y_1) \\ \vdots & \vdots & \ddots & \vdots & \vdots \\ b_{n1}^{\alpha}(y_n) & b_{n1}^{\beta}(y_n) & \dots & b_{nm}^{\alpha}(y_n) & b_{nm}^{\beta}(y_n) \end{bmatrix}, \quad (3)$$

where  $b_{jk}^{\alpha}$  and  $b_{jk}^{\beta}$  are actuator-specific, position-dependent motor gains. The right-hand side of (1) then results in a column with forces applied on the carriers, i.e.,

$$\tau = B(y)u = \begin{bmatrix} \sum_{k=1}^m \tau_{1k} & \dots & \sum_{k=1}^m \tau_{nk} \end{bmatrix}^T. \quad (4)$$

In (4),  $\tau_{jk}$  is the force applied by actuator  $k$  on carrier  $j$ , and is straightforwardly given by

$$\tau_{jk} = b_{jk}^{\alpha}(y_j)i_{\alpha,k} + b_{jk}^{\beta}(y_j)i_{\beta,k}. \quad (5)$$

Note that some elements  $\tau_{jk}$  in (4) may be zero if actuator  $k$  does not influence carrier  $j$ , which is the case when the carrier is not close enough to the actuator in order to commute.

Let us introduce the relative position of carrier  $j$  with respect to actuator  $k$ :

$$z_{jk} := y_j - Y_k, \quad (6)$$

where  $Y_k$  is the position of actuator  $k$  on the tracks, defined as the minimum position  $y_j$ , where actuator  $k$  starts influencing a carrier  $j$ , i.e.,

$$Y_k := \min \left\{ y_j \mid b_{jk}^{\alpha}(y_j) \neq 0 \vee b_{jk}^{\beta}(y_j) \neq 0 \right\}. \quad (7)$$

Note that (7) is independent of  $j$ . We are now ready to pose the following assumption regarding controllability of each carrier and similarity of the hardware components.

**Assumption 1.**  $\text{Rank}(B(y)) = n$  at all times.

**Assumption 2.** All three-phase coil segments and permanent magnet arrays are identical.

As a result of Assumption 1, any carrier at any position on the tracks is influenced by at least one actuator. A consequence of Assumption 2 is that the motor gains of each actuator  $k$  w.r.t. each carrier  $j$  are identical. We can

then simplify the motor gain matrix  $B$  in (3) by writing  $b_{jk}^{\alpha}$  and  $b_{jk}^{\beta}$  in (3) as

$$b_{jk}^{\alpha}(y_j) = b_{\alpha}(z_{jk}), \quad b_{jk}^{\beta}(y_j) = b_{\beta}(z_{jk}). \quad (8)$$

The motor gains in (8) are typically obtained from FEM-based electromagnetic simulations on the interaction between a carrier and an actuator, see [1]. By Assumption 2, we only have to perform these simulations for a single actuator/carrier interaction, simplifying the implementation of the control allocation architecture below (where the gain matrix  $B$  is explicitly used). Note that Assumption 2 is not necessarily needed for the developments in this paper, but leads to significantly reduced complexity of  $B$  and therefore easier implementation. The control allocation scheme presented below is also applicable in case the actuators are not identical.

### III. CONTROL ARCHITECTURE

In this section, the proposed control architecture is presented. We will first discuss the high-level control scheme, and subsequently the allocation algorithm.

#### A. High-level control scheme

As discussed in Section II-A, the state-of-practice control solution (which we will elaborate on in more detail in Section IV-A below) is not able to handle the control of multiple carriers by one actuator simultaneously, since the correct commutation angle for only one carrier can be obtained. We therefore propose the control allocation scheme below, that can cope with multiple carriers instead.

Consider Fig. 4. The error signals  $e$  between a reference signal  $r$  (one for each carrier on the track), and the current carrier positions  $y$  are provided to a motion controller. This controller is typically designed using well-known loop-shaping techniques, and generates the desired control forces  $\tau_c = [\tau_{c1}, \dots, \tau_{cn}]^T$ . These desired control forces should then be applied to the carriers by the AC actuators. The primary objective of the control allocator is thus to find the currents  $i_{\alpha k}$  and  $i_{\beta k}$  in the control input  $u$  in (2), such that the actuators indeed implement the desired control forces given by  $\tau_c$ . In other words, the actual forces acting on the carriers, denoted by  $\tau$  in Fig. 4, should be equal to the desired control forces coming from the motion controller, i.e.,  $\tau = B(y)u = \tau_c$ . Due to the over-actuated nature of the system, the solution to the allocation problem  $\tau = \tau_c$  (if attainable by the actuators) is not unique. We will exploit this freedom to introduce a second control objective, namely the minimization of power consumption by the actuators.

We will now discuss two allocation procedures: an unconstrained procedure, and a constrained procedure. The latter incorporates a saturation constraint on the input, which is motivated by the desire from industry to use cost-effective (less powerful) actuators.

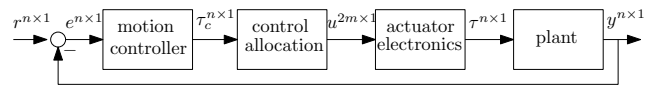


Fig. 4. High-level control architecture. The superscripts on the signals indicate their dimensions.

### B. Unconstrained control allocation

We aim at implementing the desired control force generated by the motion controller on each carrier, while minimizing the power consumption. The control allocation can then be described by the following convex quadratic programming problem (QP) [12, Ch. 4]:

$$\min_u u^\top W u, \text{ subject to } \tau_c = B(y)u, \quad (9)$$

where  $u^\top W u$  is a quadratic measure for the power consumption, and  $W$  is a symmetric weighting matrix. Since the optimization problem in (9) is convex and only contains one equality constraint, an explicit solution exists which is given by

$$u = W^{-1}B^\top(y) (B(y)W^{-1}B^\top(y))^{-1} \tau_c. \quad (10)$$

The above solution is derived from optimality conditions of (9), see, e.g., [13].

### C. Constrained control allocation

Whenever there exists a maximum allowable control input due to, e.g., cost-effective hardware design, the criterion  $\tau = \tau_c$  may not be attainable at all times. To deal with this scenario, we introduce a constraint on  $u$  in the form of a limit on the current, and the difference between the desired, and attained control forces  $s = \tau_c - \tau$ . The resulting allocation problem can then be described by a convex, quadratically constrained quadratic program (QCQP) [12, Ch. 4]

$$\min_{u,s} s^\top Q s + u^\top W u, \quad (11a)$$

subject to

$$\begin{aligned} s &= \tau_c - B(y)u, \\ i_{\alpha,k}^2 + i_{\beta,k}^2 &\leq i_{max,k}^2, \text{ for all } k \in \bar{m}. \end{aligned} \quad (11b)$$

In (11),  $W$  and  $Q$  are symmetric weighting matrices, and  $i_{max,k}$  is the current limit on actuator  $k$ . Note that choosing (the eigenvalues of)  $Q$  significantly larger than (the eigenvalues of)  $W$  prioritizes reduction of the error  $s$  over minimizing power consumption. The QCQP in (11) can be solved online using efficient algorithms as *CPLEX* [14] or *Gurobi* [15].

*Remark 1.* Although the constraint in (11b) indeed resembles a constraint on the maximum current to be provided by the actuator, we can approximate the constraint by a set of polyhedral constraints (e.g., by using separate constraints on  $i_{\alpha k}$  and  $i_{\beta k}$ ). Then, the control problem reduces to a *linear* allocation problem [8], for which efficient quadratic programming (QP) algorithms are available, e.g., active-set or interior-point methods [16], which are studied in the context of control allocation in [17], [18].

*Remark 2.* Note that finding the input  $u$  corresponds to finding the currents  $i_{\alpha j}$  and  $i_{\beta j}$  (cf. (2)). Although the actuators are often driven in the  $dq0$ -frame in industry [4, Ch. 6], we choose here to perform the control allocation in the  $\alpha, \beta$ -frame. In this way, we do not have to find an optimal commutation angle  $\theta$  for each actuator, which would appear in the above minimization problems as an extra decision variable when we would have chosen to apply

the allocation in the  $dq0$ -frame. Moreover, the motor gain matrix  $B$  in (3) would then depend on  $\theta$  as well, making the equality constraint in (9) highly nonlinear. Performing the allocation in the  $\alpha, \beta$ -frame thus significantly simplifies the control allocation problem. The optimized currents  $i_{\alpha,j}$  and  $i_{\beta,j}$  can then be transformed to the  $dq0$ -frame by the Park transformation [11, Ch. 10], after the allocation has been performed.

## IV. SIMULATION STUDY

In this section, we present a simulation study on the industrial IPMLSM-based transport system presented in Fig. 1. In particular, we show the performance improvements of the proposed control allocation strategy, compared to the state-of-practice control solution currently applied by the manufacturer.

The considered system consists of two carriers and six actuators (cf. Fig. 1), and is modeled by (1)-(3) with  $n = 2$  and  $m = 6$ . The carrier masses are  $M_1 = M_2 = 10$  kg. By the dimensions of the actuators and carriers, an actuator may influence at most two carriers. The actuators are spaced at a distance equal to the carrier length (see Fig. 3). Both the state-of-practice control strategy as the allocation strategy use a dedicated high-level (loop-shaped) motion controller for each carrier separately. For this simulation study, we use the same motion controller for both carriers, consisting of a feedback term (lead filter, integrator, and a lowpass filter), and an acceleration feedforward term. The feedback controller for carrier  $j$  formulated in the Laplace domain is given by

$$\tau_{fb,j}(s) = \frac{1.58 \cdot 10^8 s^2 + 8.6 \cdot 10^9 s + 8.31 \cdot 10^{10}}{2.11 \cdot 10^{-4} s^4 + 0.45 s^3 + 473.3 s^2 + 1.26 \cdot 10^5 s} e_j(s), \quad (12)$$

with  $s \in \mathbb{C}$ , and where  $e_j = r_j - y_j$  the position error signal of carrier  $j$ , and  $r_j$  the position reference. The acceleration feedforward term is given by  $\tau_{ff,j} = 0.9 M_j \ddot{r}_j$ , and the total control force is then given by  $\tau_{c,j} = \tau_{ff,j} + \tau_{fb,j}$ . Both strategies (i.e., the state-of-practice solution and the proposed allocation strategy) aim at implementing the desired control force for each carrier in a different manner, as we will illustrate below.

### A. State-of-practice control strategy

The state-of-practice control strategy currently used by the manufacturer operates in the  $dq0$  reference frame (see Fig. 2). By using the  $dq0$ -frame, only one control input  $i_q$  per carrier exists (because  $i_d$  is controlled to zero at all times), which is obtained by dividing the desired control force  $\tau_c$  by a *fixed* motor gain (thereby ignoring actuator end-effects), see Fig. 5. This control signal is then applied to each actuator that commutes with the considered carrier by means of a selector. However, when an actuator influences two carriers, the selector implements the control signal for the carrier *that influences the actuator the most*.

If an actuator commutes with only a single carrier, then this control strategy works well, as the actuator indeed applies the desired control force on the carrier by applying the correct commutation angle (which is a function of the carrier position). This control strategy, however, does no longer

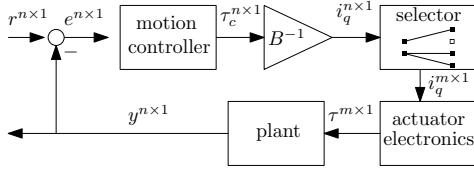


Fig. 5. State-of-practice control strategy. The superscripts on the signals indicate their dimensions.

work properly when an actuator influences two carriers. The correct commutation angle is then only applied for the most overlapping carrier, which results in a wrong commutation angle for the second carrier. As a result, there is a mismatch between the desired and implemented control force on the carrier that overlaps the actuator the least. The implications of this fact are illustrated below.

### B. Proposed allocation strategy

In contrast to the state-of-practice control strategy, the allocation scheme is applied in the  $\alpha, \beta$  reference frame. The coefficients of the position-dependent motor gain matrix  $B(y)$  in (3), (8) are obtained from FEM-based electromagnetic simulations [1] by measuring the relative position  $z_{jk}$  of carrier  $j$  with respect to actuator  $k$ . We assume that all actuators are identical, see Assumption 2. The motor gains, as a function of  $z_{jk}$ , are presented in Fig. 6, where the deterioration of the gains at both ends of the region of influence can be observed (i.e., the end-effects). The motor gain matrix is explicitly used in the allocation scheme, see (9), (10), and (11).

### C. Simulation results

We have implemented the system model (1)-(3), and both the state-of-practice and proposed allocation controller strategies. The following three scenarios are studied:

- A parallel motion of the carriers, where the relative distance between the carriers is equal to an integer times the pole-pair pitch of the magnets;
- A parallel motion of the carriers, with a reduced relative distance (not equal to an integer times the pole-pair pitch of the magnets);
- A complex motion, combining independent and adjacent carrier motion. This reference trajectory has been recorded from the setup in Fig. 1 by manually moving the carriers.

We will now discuss the results for each scenario.

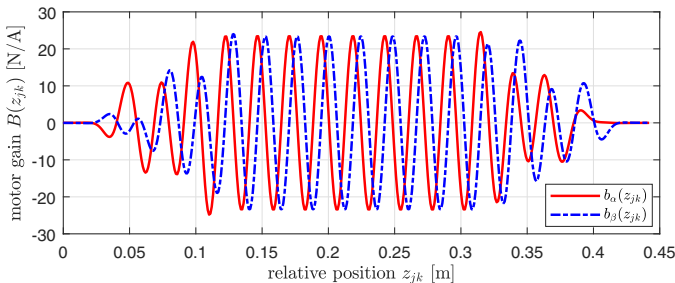


Fig. 6. Motor gains as a function of the relative position.

**Scenario a)** Consider Fig. 7a. Both carriers track the reference well when controlled by either the state-of-practice strategy, and the (unconstrained) allocation strategy of Section III-B. Due to the specific relative distance between the carriers, the actuators are able to sufficiently align for both carriers and the control force requested by the motion controller is achieved well, despite the fact that actuator 2, 3, and 4 influence both carriers (see the third subplot). Since both carriers perform the same motion profile, they require the same control forces. Then, due to the fact that the relative distance between the carriers is equal to an integer times the pole-pair pitch of the magnets, the required commutation angle of the actuator is the same. As a result, the control forces  $\tau_c$  are indeed attainable for both carriers so that both carriers are able to track the reference. As expected, the proposed control allocation strategy has equal performance to the state-of-practice control strategy in terms of accuracy in this specific scenario.

**Scenario b)** Consider Fig. 7b, where the relative distance between the carriers have been slightly decreased with respect to Scenario a). It stands out that the state-of-practice controller now results in a relatively large position error during the acceleration phase. This is caused by the fact that the shared actuators are only able to take the correct commutation angle for the most overlapping carrier. The other carrier then experiences a control force that deviates from the desired control force coming from the motion controller. In contrast, the unconstrained allocation scheme of III-B is instead able to find a control input such that the trajectory can be followed well, with only small position errors. Next, we apply the *constrained* allocation scheme of III-C to investigate the potential of the controller when less powerful actuators are used. Less powerful actuators yield economic benefits for the manufacturer, if the desired specifications in terms of accuracy are still satisfied. We take  $W = I^{2m}$ ,  $Q = 5I^n$  (with  $I$  the identity matrix), and set *separate* current saturation limits for both  $i_{\alpha,k}$  and  $i_{\beta,k}$  to 0.8 A (see Remark 1). The results are shown in red-dashed in Fig. 7b), where it can be observed that the limited attainable control force yields a local increase in position error (see the second subplot), but significantly less actuator duty (see the bottom subplots).

**Scenario c)** Consider Fig. 7c. The state-of-practice control solution is now unable to allow both carriers to follow the reference due to the mismatch in desired and implemented control force, as discussed in Scenario b). It stands out that, due to the independent motion of the carriers, this mismatch is large enough for one carrier to completely deviate from the setpoint when using the state-of-practice controller. The unconstrained allocation scheme of Section III-B results in good tracking of both carriers instead, with only a small position error. The *constrained* allocation scheme of Section III-C (with  $Q$  and  $W$  as in Scenario b), and challenging maximum values of 0.4A for both  $i_{\alpha,k}$  and  $i_{\beta,k}$ ) again results in decreased tracking performance, but significantly less actuator duty.

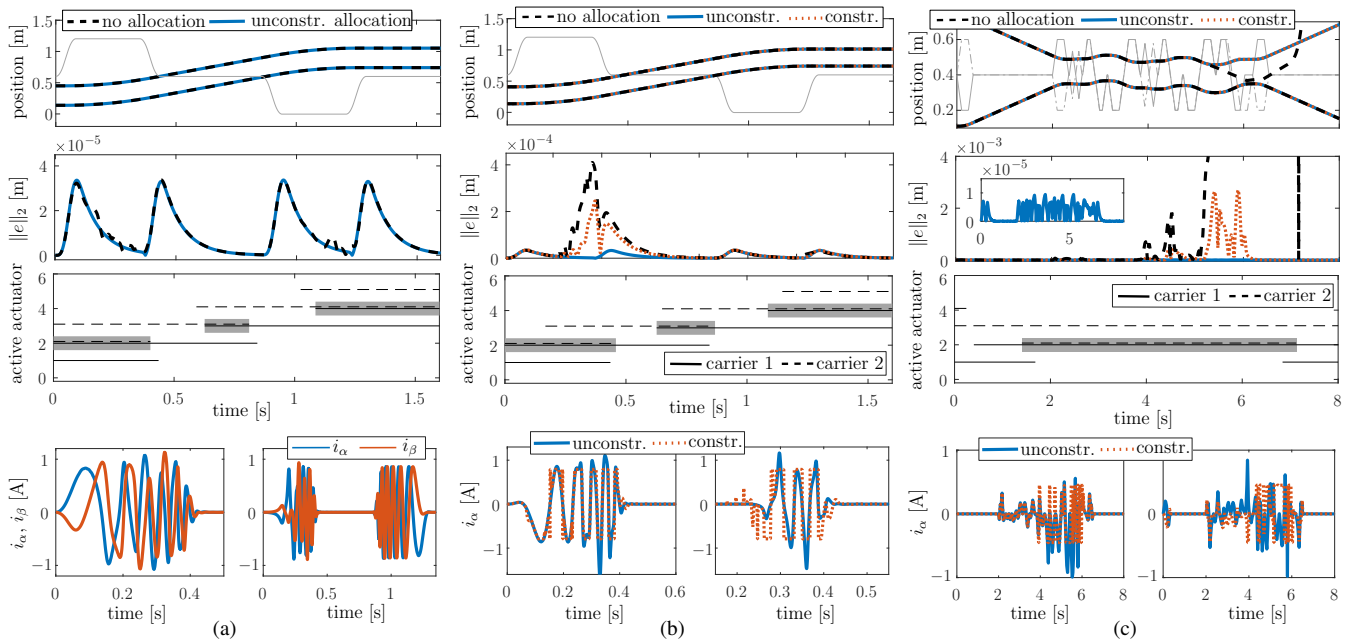


Fig. 7. Simulation results for the scenarios a, b, and c. From top to bottom: carrier position and (scaled) acceleration setpoint (gray), norm of the position error, active actuators, and illustrative input currents. The gray patches in the 3<sup>rd</sup> subplots indicate the time spans where an actuator influences both carriers for the unconstrained allocation simulations. The bottom plots show, for actuator 2 and 3, the  $\alpha, \beta$ -currents in (a), and the  $\alpha$ -currents in (b) and (c).

#### D. Discussion

The simulation study shows that the proposed control allocation scheme achieves (compared to the state-of-practice controller used by the manufacturer) 1) improved tracking performance, 2) allowing independent motion of multiple carriers while influenced by shared actuators, and 3) the possibility to take account actuator limits into account. The latter result may be used by the manufacturer to find a trade-off between achievable tracking performance and required actuator power: taking into account that less powerful actuators are often more cost-effective. An advantage of a cost-effective system design also results from the fact that the allocation scheme allows for a less strict actuator spacing. Namely, the control allocation algorithm is able to compensate for fluctuations in the motor gains due to end-effects, by adapting the control currents. In this way, the correct control force can still be implemented. The economic benefit then comes from the fact that less actuators may be placed on the tracks while still achieving a specified performance. Finally, the allocation strategy aims at minimizing the power consumption in case a carrier is over-actuated, which is not addressed by the state-of-practice control strategy.

#### V. CONCLUSIONS

We have presented a control allocation framework for an industrial translational transport and positioning system, based on an IPMLSM (inverted permanent-magnet linear synchronous motor). The proposed allocation technique results in enhanced tracking, allowing for independent motion of multiple carriers, and relaxed hardware design specifications, compared to the state-of-practice control strategy used by the manufacturer. Moreover, the allocation framework is able to take into account actuator limitations. We have

illustrated the benefits of the proposed control allocation strategy by means of a simulation study.

#### REFERENCES

- [1] J. Rovers, J. Jansen, and E. Lomonova, "Novel force ripple reduction method for a moving-magnet linear synchronous motor with a segmented stator," in *Int. Conf. Electrical Machines and Systems*, 2008, pp. 2942–2947.
- [2] "Industrial applications of an IPMLSM." [Online]. Available: <http://www.boschrexroth.com/lms>
- [3] I. Boldea and S. Nasar, "Vector control of AC drives." Orlando, FL: CRC Press, 1992.
- [4] J. Gieras, Z. Piech, and B. Tomczuk, *Linear synchronous motors*, 2nd ed. Boca Raton, FL: CRC Press, 2012.
- [5] H. Beaty and J. Kirtley, *Electric motor handbook*. New York: McGraw-Hill, 1998.
- [6] K. Zhou, J. Doyle, and K. Glover, *Robust and optimal control*. New Jersey: Prentice Hall, 1996.
- [7] O. Härkegård and S. T. Glad, "Resolving actuator redundancy - optimal control vs. control allocation," *Automatica*, vol. 41, no. 1, pp. 137–144, 2005.
- [8] T. Johansen and T. Fossen, "Control allocation - a survey," *Automatica*, vol. 49, no. 5, pp. 1087–1103, 2013.
- [9] B. Anderson and J. Moore, *Optimal control: linear quadratic methods*. New Jersey: Prentice Hall, 1990.
- [10] J. Maciejowski, *Predictive control with constraints*. Pearson Education, 2001.
- [11] H. Toliyat and S. Campbell, *DSP-based electromechanical motion control*. Boca Raton, FL: CRC Press, 2003.
- [12] S. Boyd and L. Vandenberghe, *Convex Optimization*. New York: Cambridge University Press, 2004.
- [13] K. Bordignon and W. Durham, "Closed-form solutions to constrained control allocation problem," *J. Guidance, Control, and Dynamics*, vol. 18, no. 5, pp. 1000–1007, 1995.
- [14] "CPLEX Optimizer." [Online]. Available: <https://www.ibm.com/analytics/data-science/prescriptive-analytics/cplex-optimizer>
- [15] "Gurobi optimization." [Online]. Available: <http://www.gurobi.com/>
- [16] J. Nocedal and S. Wright, *Numerical optimization*, 2nd ed. New York: Springer, 2006.
- [17] O. Härkegård, "Efficient active set algorithms for solving constrained least squares problems in aircraft control allocation," *Proc. 41th IEEE conf. decision and control*, vol. 2, pp. 1295–1300, 2002.
- [18] J. Petersen and M. Bodson, "Interior-point algorithms for control allocation," *J. Guidance, Control, and Dynamics*, vol. 28, no. 3, pp. 471–480, 2005.